Canadian Mineralogist
Vol. 25, pp. 717-730 (1987)

OCCUPANCY OF T SITES IN THE SCAPOLITE SERIES: A MULTINUCLEAR NMR STUDY USING MAGIC-ANGLE SPINNING

BARBARA L. SHERRIFF AND H. DOUGLAS GRUNDY
Department of Geology, McMaster University, Hamilton, Ontario L8S 4L8

J. STEPHEN HARTMAN
Department of Chemistry, Brock University, St. Catharines, Ontario L2S 3A1

ABSTRACT

Magic-angle spinning (MAS) nmr spectra were obtained for ^{29}Si, ^{27}Al, ^{23}Na and ^{13}C in a series of scapolite samples covering the whole range of naturally occurring compositions. The ^{29}Si peaks are assigned to specific tetrahedral configurations from calculations of peak positions based on a modification of the semi-empirical formula of Janes & Oldfield (1985). A model for Al–Si ordering of the framework has been developed from the original X-ray refinements of the structures, which determines the composition of the anion–cation clusters in the framework cavities. This model is consistent with the peak positions and relative intensities of the ^{29}Si MAS nmr spectra and explains ^{23}Na and ^{27}Al nmr spectra.

Keywords: scapolite, nuclear magnetic resonance, magic-angle spinning, Al–Si ordering.

SOMMAIRE

On décrit les spectres de résonance magnétique nucléaire que l'on obtient par spinning à l'angle magique pour ^{29}Si, ^{27}Al, ^{23}Na et ^{13}C dans une série d'échantillons de scapolite qui représentent les compositions naturelles. Les pics ^{29}Si sont attribués à des configurations tétraédriques spécifiques, en utilisant les positions calculées de ces pics d'après une modification de la formule semi-empirique de Janes & Oldfield (1985). On a dévelopé un modèle pour la mise en ordre Al–Si de la charpente à partir des données structurales originelles déterminées aux rayons X. Ce modèle prédit la composition des groupements d'anions et de cations dans les cavités de la charpente. Il concorde avec la position des pics pour le spectre de ^{29}Si, ainsi que leurs intensités relatives, et parvient à rendre compte des spectres de ^{23}Na et ^{27}Al.

(Traduit par la Rédaction)

Mots-clés: scapolite, résonance magnétique nucléaire, spinning à l'angle magique, mise en ordre Al–Si.

INTRODUCTION

Nuclear magnetic resonance spectroscopy using the technique of magic-angle spinning (MAS nmr) is an important tool in the study of crystal structures and has been applied extensively to the study of synthetic zeolites (Fyfe *et al.* 1983, 1984) and to mineral systems such as clays (Barron & Frost 1985) and feldspars (Sherriff & Hartman 1985, Kirkpatrick *et al.* 1985). Here we report on the use of MAS nmr to determine variations in the degree of Al–Si order in the scapolite series of minerals.

Scapolite is a framework aluminosilicate; compositions define a solid-solution series with end members *marialite*, $Na_4Al_3Si_9O_{24}Cl$, and *meionite*, $Ca_4Al_6Si_6O_{24}CO_3$. Between 0 and 75% meionite (*Me*), the substitution involves $Ca_3Al_2CO_3$ for Na_3Si_2Cl, but from 75% to 100% meionite it involves CaAl for NaSi (Lin 1971). The three tetrahedral (*T*) sites in the scapolite structure contain silicon or aluminum. The *T2* and *T3* sites are geometrically identical in the $I4/m$ space group but differ slightly in position in the $P4_2/n$ space group. Considerable interest in scapolite has been generated by the proposal that meionite scapolite is a reservoir for CO_2 in the lower crust (Newton & Goldsmith 1975).

A number of crystal-structure refinements has been reported on scapolite, covering a range of meionite contents. Those refined with the $I4/m$ space group are 19.4% *Me* (Papike & Zoltai 1965), 70.1% *Me* (Papike & Stephenson 1966), and 77% *Me* (Peterson *et al.* 1979), as well as a synthetic sulfate-free sample with a composition of 84% *Me* (Aitkin *et al.* 1984). Lin & Burley used the $P4_2/n$ space group for the refinement of samples containing 19.4% *Me* (1973a), 93% *Me* (1973b) and 52% *Me* (1975), as did Levien & Papike (1976) for a 33.5% *Me* sample. Levien & Papike also studied thermal effects on this scapolite sample up to 1000°C.

The X-ray data allow calculation of average site-occupancies. Solid-state high-resolution nuclear magnetic resonance (nmr) based on the technique of magic-angle spinning can be used to study atomic environments in terms of next-nearest neighbors. Thus information about cation ordering can be obtained directly.

EXPERIMENTAL

MAS nmr spectra were obtained on a series of powdered scapolite samples with compositions from 21 to 93% Me, covering the entire range of natur-

TABLE 1. SCAPOLITE SAMPLES STUDIED

Sample #	%Me	Rock Type	Locality	
ON9	21.3	syenite pegmatite	Gooderham, Ont.	*
TANZ	29.5	hbl.px.granulite	Morongoro, Tanzania.	**
ON7	33.3	calcareous gneiss	Monmouth Twp., Ont.	*
GL	34.1	marble	Gib Lake, Pontiac Twp., Ont.	*
ON70	39.5	-	MpWapwa, Tanzania.	*
CA63A	44.5	pegmatitic skarn	Grand Calumet Twp., QC	**
MAD	45.2	-	Madagascar	**
Q26	48.2	pegmatitic skarn	Clapham Twp, QC	*
Q13	51.3	px. gneiss	Huddersfield Twp., Ont.	*
MIN	56.8	skarn	Minden, Ont.	**
ON27	59.3	pegmatitic skarn	Olmsteadville, N.Y.	*
Q85	65.2	pegmatitic skarn	Huddersfield Twp., QC	*
BOLT	69.5	marble pegmatite	Bolton, Mass.	**
ON47	79.6	calc-silicate schist	Slyudyanka, USSR	*
MONT	91.3	vugs in marble?	Mount Vesuvius, Italy.	**

* Donated by Prof. D.M. Shaw, McMaster University.Chemical composition from Evans et al. (1969). Localities from Shaw (1960a, b).

** Donated by D. Moecher, University of Michigan.Compositions from D. Moecher (pers. commun.).

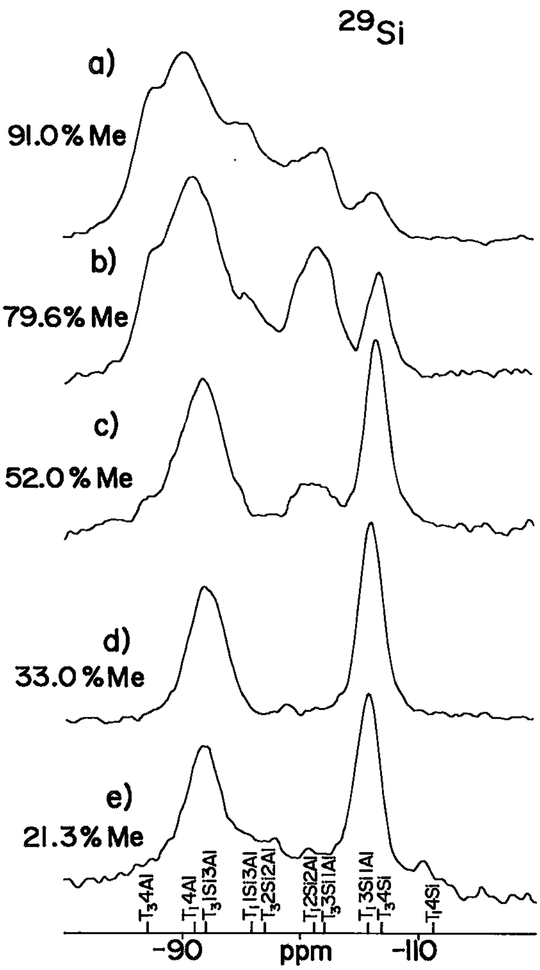

FIG. 1. ^{29}Si MAS nmr spectra of scapolite samples: (a) MONT (91.0% *Me*), (b) ON47 (79.6% *Me*), (c) Q13 (52% *Me*), (d) ON7 (33.0% *Me*), (e) ON8 (21.3% *Me*).

ally occurring compositions (Table 1). A magic-angle-spinning probe (Fyfe *et al.* 1982) with Delrin rotors was used with (i) a Bruker WH-400 multinuclear Fourier Transform nmr spectrometer equipped with a 9.4-Tesla superconducting magnet and (ii) a Bruker CXP-200 spectrometer with a 4.7-Tesla superconducting magnet. The samples were spun at approximately 3500 Hz at an angle of 54.7° to the magnetic field.

The ^{29}Si MAS nmr spectra were recorded at a frequency of 79.46 MHz on the Bruker WH-400 instrument, with 8000 data points using a spectral width of 25000 Hz, 30° pulses and a 5-s relaxation delay between pulses. A range of relaxation delays from 0.1 to 30 s was tried on three samples ON7, ON70 and ON47, but no difference in resolution was observed with relaxation delay, in contrast to the findings of Sherriff & Hartman (1985) on certain samples of feldspar. The ^{29}Si MAS nmr spectra were also recorded on the Bruker CXP-200 instrument at 38.73 MHz with 30° pulses and a 5-s delay between scans. Chemical shifts were found to be reproducible to ± 0.1 ppm on both instruments and are reported in parts per million of the magnetic field with reference to tetramethylsilane (TMS).

The ^{27}Al and ^{23}Na MAS nmr spectra were recorded on the Bruker WH-400 instrument at 104.23 and 105.80 MHz, respectively with 15° pulses and a 0.3-s relaxation delay between pulses. The chemical shifts of ^{23}Na were measured with reference to a 0.1 M aqueous solution of NaCl, and those of ^{27}Al, with reference to $[Al(H_2O)_6]^{3+}$ in a saturated aqueous solution of $Al(ClO_4)_3$. The ^{13}C MAS nmr spectra were recorded on the Bruker CXP-200 instrument at 50.32 MHz, with 30° pulses and relaxation delays between pulses ranging from 5 to 60 s, to achieve optimum strength of the signal.

The complex ^{29}Si spectra were deconvoluted using a least-squares iterative curve-fitting program written for the deconvolution of Lorentzian peaks. Relative intensities of the ^{29}Si peaks were found from the curve-fitting program and also by cutting out individual peaks from the plot and weighing them. Both methods gave similar accuracy and reproducibility for the simple spectra, but the weighing technique was judged to be impractical for spectra with many overlapping peaks. These results were compared to values calculated from the predicted occupancy of each environment.

RESULTS

The ^{29}Si MAS nmr spectra of scapolite vary considerably with meionite content. In samples between 33 and 40% *Me*, there are only two peaks (Fig. 1, Table 2), at -106 and -92 ppm. Sample ON8 (21.3% *Me*) has the same two peaks plus unresolved intensity maxima at -96 and -110 ppm. As the meionite content increases beyond 45% *Me*, the high-field peak at -106 ppm diminishes in size, and the absorption around -100 ppm increases. At the higher meionite content [79% (ON47) and 91% *Me* (MONTE)], extra low-field peaks appear at -88 ppm, and the -106 and -100 ppm peaks diminish in size relative to the peak at -96 ppm.

The ^{27}Al MAS nmr spectra of scapolite consist of one broad asymmetric peak at 58.0 ± 0.5 ppm in the tetrahedral region (Fig. 2, Table 3). There is a steady increase in peak width with increasing content of meionite (Fig. 3) as the concentration of aluminum and, hence, the number of different aluminum environments increase. There is an additional increase of approximately 200 Hz at about 45% *Me* over and above that due to the increase in number of aluminum environments.

The ^{23}Na MAS nmr spectra of scapolite all consist of very broad lines with maxima between 21 ppm and 23 ppm (Fig. 4, Table 4). The spectra of ON7 (33.3% *Me*), GL (34.1% *Me*) and CA63A (44.5% *Me*) all have a shoulder at approximately 28 ppm (Fig. 4b). This is present but not as pronounced in ON70 (39.5% *Me*) and Q26 (48.2% *Me*).

Scapolite gives a very weak ^{13}C spectrum, consisting of one broad peak at 165 ± 1 ppm. The large error in chemical shift is due to the overlapping peak from the "Delrin" rotor (Fig. 5, Table 5).

DISCUSSION

Scapolite structure

In the scapolite structure refined in space group $P4_2/n$, three types of tetrahedral (*T*) sites containing silicon or aluminum form four-membered rings, either consisting of *T*1 sites or of alternating *T*2 and *T*3 sites perpendicular to the *c* axis (Fig. 6). The *T*2–*T*3 four-membered rings are joined parallel to the *c* axis to form chains that are linked to the *T*1 rings and that form a series of five-membered rings (Fig. 7). This rigid framework has large voids, which contain four sodium or calcium cations and one chloride, carbonate or sulfate anion.

One structure in the scapolite series with perfect Al–Si ordering has been inferred to occur from X-ray data at a composition of 37% *Me* (Lin 1971, Levien & Papike 1976). In this structure, the *T*2 site contains only aluminum, and the *T*1 and *T*3 sites contain only silicon. With less aluminum (0–37% *Me*), aluminum and silicon become disordered between *T*2 and *T*3 sites, but the *T*1 site contains only silicon. In the more aluminous compositions (37–100% *Me*), aluminum and silicon become progressively distributed over all three *T* sites, with a theoretical 50% occupancy of aluminum in each site in end-member *Me* (Lin 1971). Lowenstein's rule (1954) that Al–O–Al linkages are unstable in aluminosilicates cannot be obeyed in scapolite with greater than 37% *Me*, as the five-membered rings do not allow for complete alternation of aluminum and silicon (Lin 1971).

TABLE 2. ^{29}Si MAS nmr PARAMETERS FOR SCAPOLITE

Sample	%Meionite	Peak Positions (ppm)							
ON9	21.3	-88.9,	-91.8,	-95.4,	-98.0,	-100.8,	-105.8,	-110.6	
TANZ	29.5	-91.4,	-91.9,	-92.5,	-97.7,	-102.4,	-105.8,	-106.1	-110.5
ON7	33.3		-92.0				-106.2		
GL	34.1		-92.1				-106.2		
ON70	39.5		-92.1			-100.8,	-106.3		
CA63A	44.5	-87.9,	-92.0,	-92.4,			-106.2		
MAD	45.2	-90.9,	-91.6,	-92.4,	-101.0,	-105.7,	-106.1,	-106.6	
Q26	48.2	-88.1,	-91.9,	-92.3,	-100.2,		-106.4		
Q13	51.3	-87.3,	-91.6,	-95.3,	-101.0,	-102.6,	-106.4		
MIN	56.8	-91.1,	-92.8,	-95.5,	-101.5,		-106.1,	-106.4	
ON27	59.3	-89.0,	-91.7,	-98.9,	-101.0,	-102.8,	-106.8,		
Q85	65.2	-87.6,	-91.5,	-99.2,	-101.2,	-102.7,	-106.5,		
BOLT	69.5	-86.6,	-90.9,	-92.7,	-100.5,	-102.3,	-106.1,	-106.9	
ON47	79.6	-87.6,	-90.8,	-99.6,	-101.6,	-102.7,	-106.7,		
MONT	91.3	-87.2,	-90.5,	-95.6,	-101.9,		-106.7		

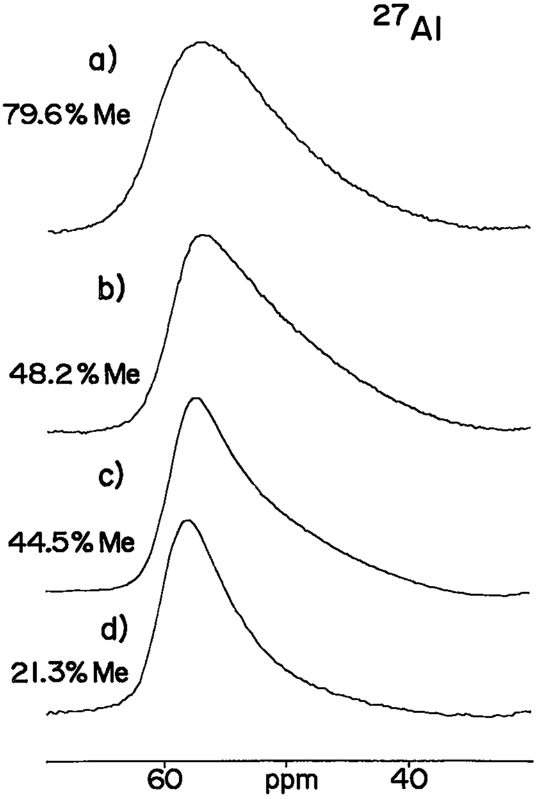

FIG. 2. ^{27}Al MAS nmr spectra of scapolite samples: (a) ON47 (79.6% *Me*), (b) Q26 (48.2% *Me*), (c) CA63A (44.5% *Me*), (d) ON8 (21.3% *Me*).

A further source of variability in degree of order in scapolite relates to occupancy of the voids. Chamberlain *et al.* (1985) estimated from energy calculations that the most stable arrangement is one with a maximum number of sodium ions around chloride and of calcium ions around carbonate. This arrangement would give predominantly Na_4Cl and Ca_4CO_3 configurations, with excess charges of +3 and +6, respectively. However, the clusters of cations and anions in the voids are related to Al–Si ordering of the framework in order that excess charge can be balanced locally. In the ordered framework of 33% *Me*, there are four aluminum ions, each contributing a negative charge in the *T*2 sites around each void. Therefore, to obtain a charge balance the configurations of Na_3CaCl and $Na_2Ca_2CO_3$ are considered to be the most favorable, as both of these have an excess charge of +4.

TABLE 3. ^{27}Al MAS nmr PARAMETERS FOR SCAPOLITE

Sample	%Meionite	Peak Position (ppm)	Peakwidth at half height (Hz)
ON9	21.3	58.2	680
TANZ	29.5	57.9	830
ON7	33.3	57.9	780
GL	34.1	57.9	880
ON70	39.5	57.7	970
CA63A	44.5	57.9	820
MAD	45.2	58.0	880
Q26	48.2	57.6	1110
Q13	51.3	57.5	1120
MIN	56.8	57.6	1140
ON27	59.3	57.6	1170
Q85	65.2	57.9	1180
BOLT	69.5	57.5	1120
ON47	79.6	57.4	1250
MONT	91.3	57.3	1250

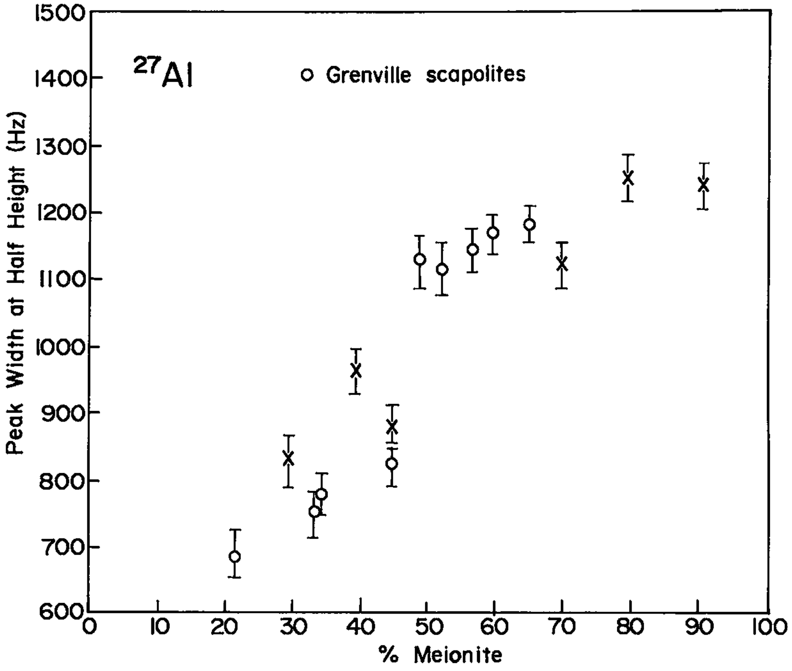

FIG. 3. A graph of ^{27}Al peak width plotted against meionite content.

We have calculated cage configurations for scapolite samples from 21% to 91% *Me* from their chemical compositions (Evans *et al.* 1969) and for stoichiometric compositions for 0, 37, 50, 75 and 100% *Me*, assuming that the configurations with +4 charge are the most favored (Table 6). For less than 33% *Me*, the excess ions form Na_4Cl groups, which can be balanced by cages with only three aluminum ions. Above 37% *Me*, $NaCa_3CO_3$ and Ca_4CO_3 configurations are necessary to use up the excess ions, but in these compositions the +6 charge can be balanced by aluminum in the *T*1 sites. The discrepancy between theoretical and calculated values is due to the fact that scapolite compositions rarely are stoichiometric.

Silicon-29 MAS nmr

^{29}Si MAS nmr chemical shifts of aluminosilicates were originally correlated with degree of condensation of the silicon-oxygen tetrahedra (*i.e.*, whether the structures are framework, sheet, chain, *etc.*) and with number of aluminum next-nearest neighbors (Lippmaa *et al.* 1980, 1981). The nature of the next-nearest-neighbor tetrahedral cation causes a large variation in the ^{29}Si and ^{27}Al chemical shift in aluminosilicates (Magi *et al.* 1984, Lippmaa *et al.* 1986). Therefore, the type and occupancy of neighboring *T* sites are of paramount importance in spectral interpretations. *T*1 sites are connected through bridging oxygen atoms to two other *T*1, one *T*2 and one *T*3 sites. *T*2 sites have one *T*1 and three *T*3 neighbors, and *T*3 sites, one *T*1 and three *T*2 neighbors (Figs. 6, 7).

Recently, the angular distortion of the SiO_4 tetrahedra, the Si–O–*T* angle, the identity of other neighboring cations and the sigma orbital hybridization have been correlated with chemical shift (Magi *et al.* 1984).

Radeglia & Engelhardt (1985) and Janes & Oldfield (1985) proposed two different semi-empirical formulae for the calculation of ^{29}Si chemical shift of silicates. The formula of Radeglia & Engelhardt (1985) for framework aluminosilicates uses the mean Si–O–*T* angle and adds 5 ppm for each next-nearest-neighbor ^{IV}Al, whereas that of Janes & Oldfield (1985) uses the "group electronegativity" (EN) of next-nearest-neighbor aluminum and silicon ions and of all other cations in the chemical formula. The value of EN is calculated from other nmr spectra. This allows the formula to be used for all aluminosilicates, not just for tectosilicates. Janes & Oldfield adjusted the EN(OSi) term to allow for the effect of varying the Si–O–Si angle.

Chemical shifts of ^{29}Si were calculated using both of these formulae for *T*1 (3Si1Al) and *T*3 (1Si3Al) sites of scapolite with 19.4% *Me* (Lin & Burley 1973a), 34% *Me* (Levien & Papike 1976), 52% *Me* (Lin & Burley 1975), 70.1% *Me* (Papike & Stephenson 1966) and 93% *Me* (Lin & Burley 1973b). The discrepancy between the calculated and measured chemical shifts, especially for the more aluminous material (Fig. 8), leads us to produce a modification to the formula of Janes & Oldfield (1985) to allow for the effect of varying the Si–O–Al angle on the group electronegativity of aluminum. This was calculated using the measured value of –106.2 ppm for the *T*1 (3Si1Al) site of sample GL (34% *Me*).

$$\mathrm{EN(OAl)} = (\text{mean Si–O–Al}/138.41) + 2.734$$

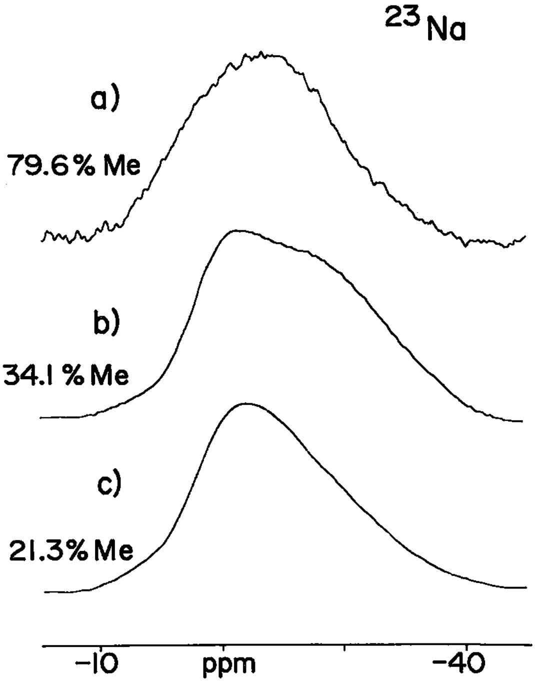

FIG. 4. ^{23}Na MAS nmr spectra of scapolite samples: (a) ON47 (79.6% *Me*), (b) GL (34.1% *Me*), (c) ON8 (21.3% *Me*).

TABLE 4. ^{23}Na MAS nmr PARAMETER FOR SCAPOLITE

Sample	%Meionite	Peak Position (ppm)		Peakwidth at half height (Hz)
ON9	21.3	-14.7		1460
TANZ	29.5	-14.7		1480
ON7	33.3	-13.8,	-19.7	1680
GL	34.1	-13.4,	-19.4	1760
ON70	39.5	-13.5,	-20.6	1680
CA63A	44.5	-13.8,	-21.7	1590
MAD	45.2	-14.7,	-21.0	1630
Q26	48.2	-14.7		1590
Q13	51.3	-14.8		1570
MIN	56.8	-15.3		1620
Q85	65.2	-15.4		1540
BOLT	69.5	-14.4,	-22.0	2260
ON47	79.6	-15.8		1600
MONT	91.3	-15.7		2300

The above modification was then used with the Janes & Oldfield (1985) formula to calculate the chemical shift of *T* sites from the same X-ray data for the three *T* sites with all possible combinations of Al–Si next-nearest neighbors (Table 7). These values of *T*1(3Si1Al) and *T*3(1Si3Al) correlated better with the measured values than previous calculations using the unmodified formulae, and so these values were used to assign silicon sites to ^{29}Si nmr peaks (Fig. 1).

The measured and calculated values of *T*1(3Si1Al) chemical shift diverge in the case of scapolite with greater than 34% *Me*, for all three formulae (Fig. 8). The calculations rely on the *T*1–O–Si angles from the X-ray data, which are an average for all *T*1 sites containing both aluminum and silicon, whereas the nmr peaks are produced by only the silicon sites. For compositions of less than 33% *Me*, and therefore without aluminum in the *T*1 sites, chemical shifts are

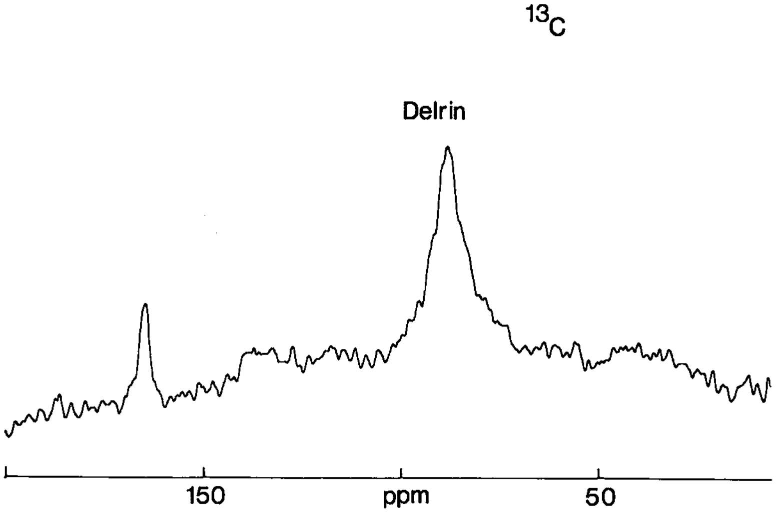

FIG. 5. ^{13}C MAS nmr spectrum of scapolite sample Q13 (52% *Me*). The sample holders are made of 'Delrin'.

TABLE 5. ^{13}C PARAMETERS FOR SCAPOLITE

Sample	% Meionite	Peak Position (ppm)
ON9	21.3	
ON7	33.3	
GL	34.1	165.2
ON70	39.5	165.0
CA63A	44.5	163.8
Q26	48.2	165.9
Q13	52.0	165.1
ON27	59.3	165.8
Q85	65.2	166.3
ON47	79.6	166.4
calcite		167.5
magnesite		169.1
aragonite		169.9
dolomite		167.7

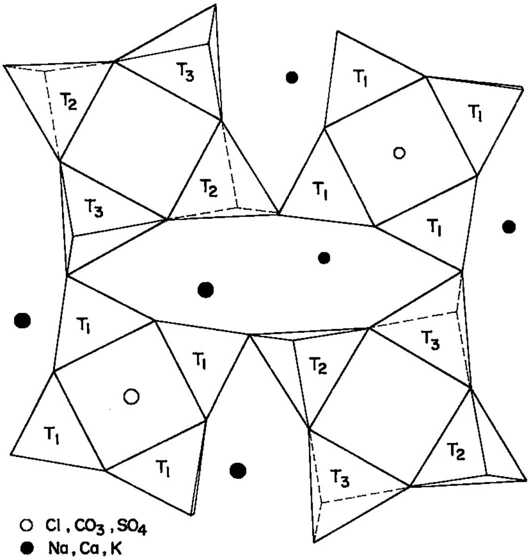

FIG. 6. The structure of scapolite viewed along the *c* axis.

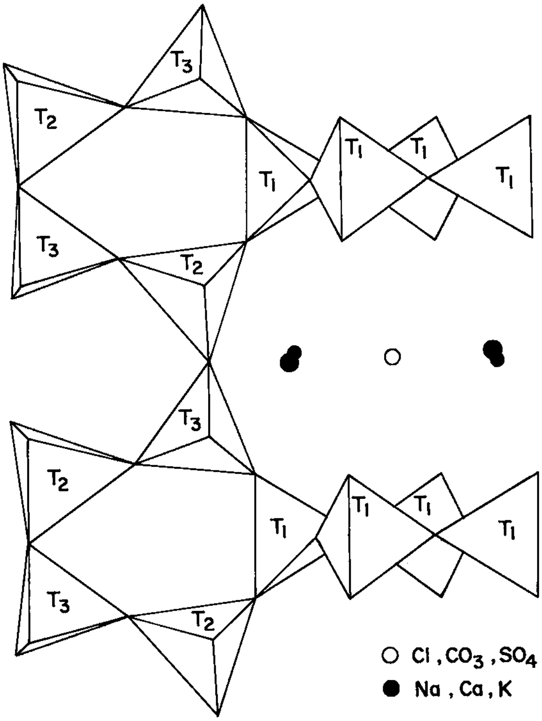

FIG. 7. The structure of scapolite viewed along the *a* axis.

parallel to the calculated values. Distortion of the *T*1 tetrahedra occurs when aluminum replaces silicon, with expansion along the *a* dimension, whereas the *c* dimension remains unchanged. The *T*–O–*T* angles also change, which leads to an increase in the calculated values of chemical shift. As the observed values of ^{29}Si chemical shift change very little with meionite content, the change of the *T*–O–*T* angles must be confined to the aluminum-containing *T*1 sites.

There is very little discrepancy, using our formula, between the measured and calculated values of chemical shifts for the *T*2 or *T*3 sites. There is no net increase of aluminum in the *T*2 and *T*3 site past 37% *Me* (Lin 1971). The change in the *T*–O–*T* angles, which is reflected in the calculated values of chemical shift, is therefore present in both aluminum- and silicon-containing sites, in contrast to the situation with *T*1.

TABLE 6. CALCULATED POPULATIONS OF CATIONS IN SCAPOLITE CAVITIES

Sample	%Meionite	Na4Cl	Na3CaCl	Na2Ca2CO3	$Na_2Ca_2SO_4$	Ca_4CO_3	Ca_4SO_4
	0	1.0	-	-	-	-	-
ON9	21.3	.35	.37	.22	-	-	-
TANZ	29.5	.20	.50	.23	.074	-	-
ON7	33.3	-	.61	.30	.019	-	-
GL	34.1	-	.58	.38	-	-	-
	37.0		.5	.5	-	-	-
ON70	39.5	-	.46	.44	.063	-	.021
CA63A	44.5	-	.41	.49	-	-	.093
MAD	45.2	-	.46	.42	-	.050	.060
Q26	48.2	-	.38	.46	-	.12	.026
	50	-	.33	.50	-	.16	-
Q13	51.3	-	.36	.41	-	.20	.10
MIN	56.8	-	.30	.44	-	.12	.13
ON27	59.3	-	.26	.41	-	.32	-
Q85	65.2	-	.21	.37	-	.18	.16
BOLT	69.5	-	.12	.44	-	.44	-
	75.0	-	-	.33	-	.67	-
ON4	79.6	-	.080	.39	-	.28	.24
MONT	91.3	-	.064	.28	-	.78	.02
	100.0	-	-	-	-	1.0	.02-

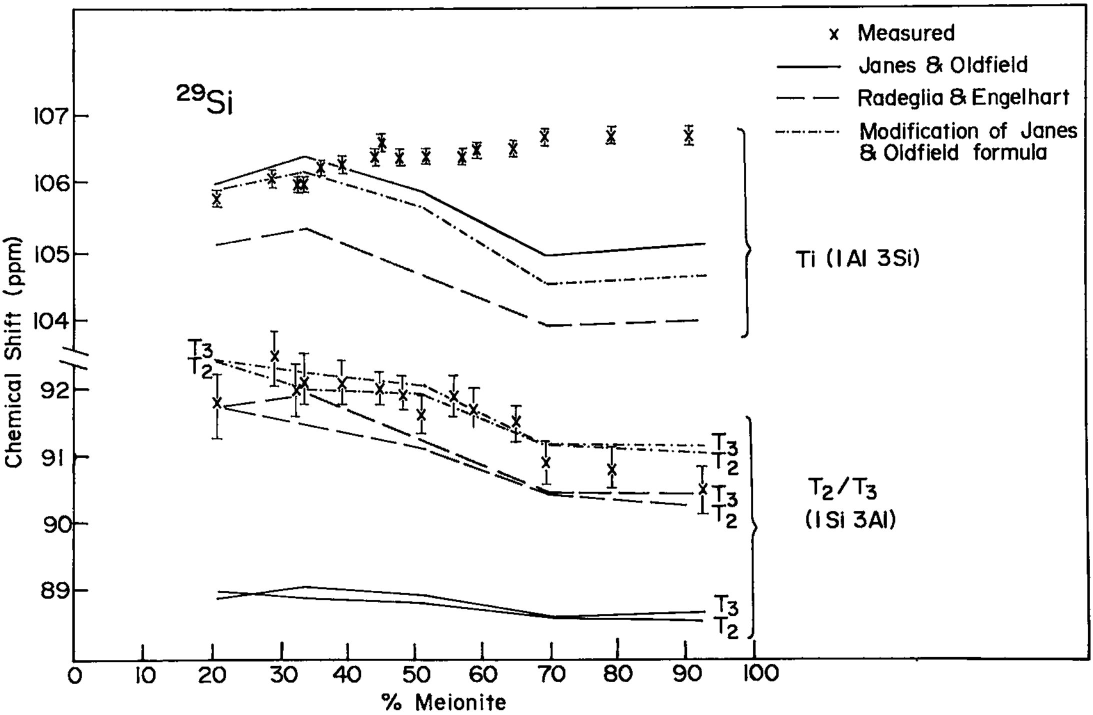

FIG. 8. A graph of ^{29}Si chemical shift, both calculated and measured against meionite content for *T*1(3Si1Al), *T*2(1Si3Al) and *T*3(1Si3Al) configurations.

As there is less than 0.1 ppm difference between the calculated values of equivalent *T*2 and *T*3 sites, they are considered together in our interpretation of the spectra and designated *T*2–*T*3.

Deconvolution of the ^{29}Si spectra indicates that even the simple two-peak spectrum of the ordered structure at 33% *Me* contains at least two absorptions giving rise to each peak (Fig. 9). Since there are only two Al–Si configurations possible in this structure, *T*1(3Si1Al) and *T*3(1Si3Al), the division into further peaks is the effect of the placement of sodium or calcium as adjacent cations. Magi *et al.* (1984) reported that replacing sodium by calcium produces a shift to high field in the adjacent silicon atoms. This effect could be considerable, *e.g.*, 8.8. ppm (Grobet *et al.* 1985).

The *T*1 site is farther from the nearest Na or Ca

TABLE 7. CALCULATED VALUES OF CHEMICAL SHIFT IN SCAPOLITE

% Meionite	4Si	3Si1Al	2Si2Al	1Si3Al	4Al
T1					
21.3	-110.8	-105.9	-101.0	-96.1	-91.1
34.1	-111.1	-106.2	-101.3	-96.3	-91.4
52.0	-110.6	-105.7	-100.7	-95.8	-90.9
70.1	-109.4	-104.5	-99.6	-94.6	-89.7
93.0	-109.5	-104.6	-99.6	-94.7	-89.8
T2					
21.3	-107.2	-102.3	-97.4	-92.4	-87.5
34.1	-106.7	-101.8	-96.9	-91.9	-87.1
52.0	-106.7	-101.8	-96.8	-91.9	-87.0
70.1	-105.9	-101.0	-96.1	-91.2	-86.2
93.0	-105.8	-100.9	-96.0	-91.0	-86.2
T3					
21.3	-107.2	-102.2	-97.3	-92.4	-87.5
34.1	-107.0	-102.0	-97.1	-92.2	-87.3
52.0	-106.8	-101.8	-96.9	-92.0	-87.1
70.1	-105.9	-101.0	-96.1	-91.2	-86.2
93.0	-105.9	-101.0	-96.1	-91.1	-86.3

cation than is the *T*3 site; hence the effect on the *T*1 site is minor. As a result, peaks for the *T*1 site are closer, producing a sharper combined peak than the combined peaks for the *T*3 site, despite the fact that both the combined peaks have the same intensity. The chemical shift of the *T*1(3Si1Al) peak shifts slightly to high field with meionite content, from -105.7 ppm at 21% *Me* to -106.7 ppm at 91% *Me*. This shift apparently is due to the increase in number of Si sites adjacent to calcium and, hence, an increase in relative intensity of the high-field peak.

If (i) the five possible Al–Si next-nearest-neighbor configurations and (ii) the effect of Na or Ca as adjacent cation are considered for each of the three

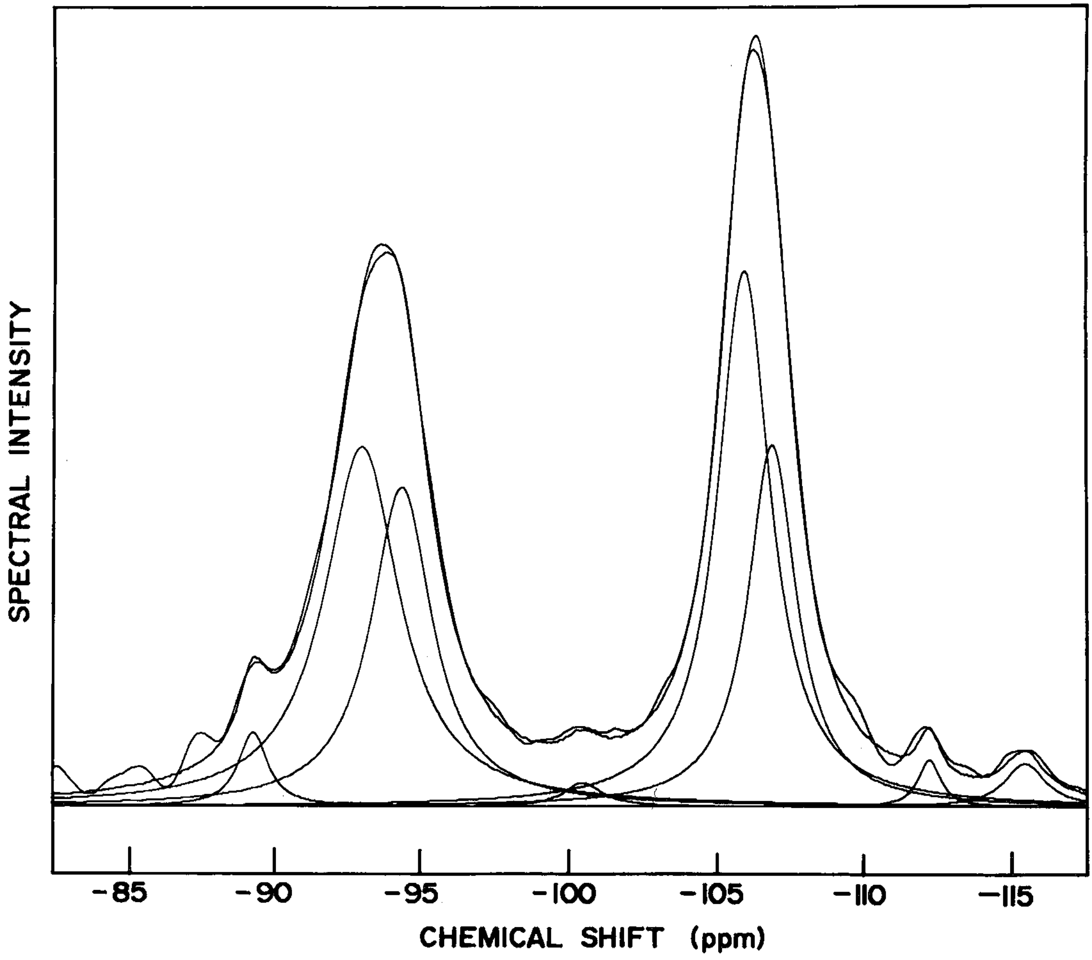

FIG. 9. Deconvolution of the ^{29}Si MAS nmr spectrum of GL (34.1% *Me*) using a least-squares iterative program used to fit Lorentzian peaks.

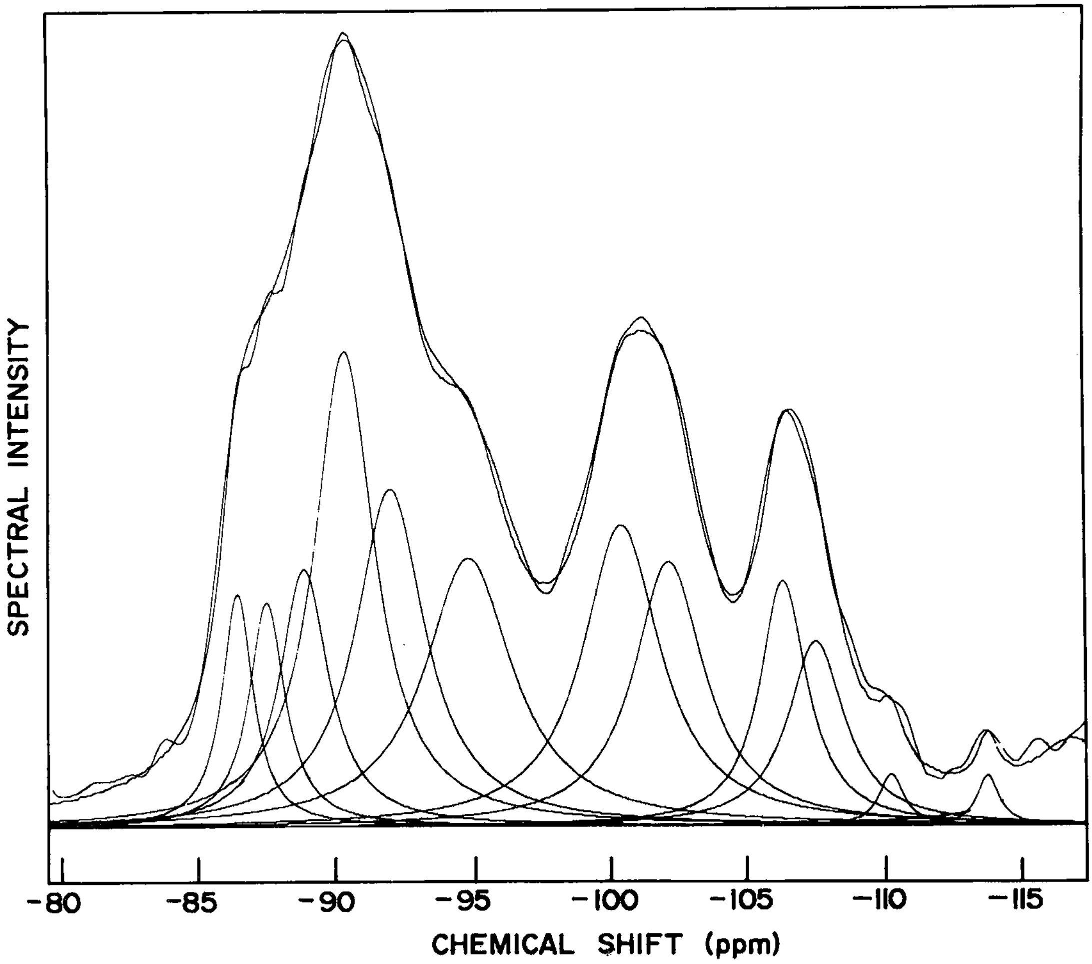

FIG. 10. Deconvolution of the ^{29}Si MAS nmr spectrum of ON47 (79.6% *Me*).

T sites, then there are 30 possible ^{29}Si environments. Deconvolution of the broad envelopes of resonances in the spectrum of a scapolite with a high meionite content shows many of the expected peaks (Fig. 10). However, the credibility given to the relative intensity and position of these fitted peaks must decrease with number of peaks fitted.

A charge-balanced structure of scapolite with 33% *Me* requires two types of cavity clusters, Na_3CaCl and $Ca_2Na_2CO_3$, both with a charge of +4, which is balanced by the charge of four surrounding AlO_4^{5-} tetrahedra in the *T*2 site (Fig. 11). This structure, with all of the Al in the *T*2 site and the *T*1 and *T*3 sites occupied by silicon, contains two silicon configurations, *T*1(3Si1Al) and *T*3(1Si3Al), which give ^{29}Si nmr peaks at -106 and -92 ppm. The *T*2-*T*3 chains of four-membered rings comprise alternating *T*2 sites, populated by Al, and *T*3 sites, by Si.

Below 33% *Me*, the *T*1 sites contain only silicon, with excess Si entering the *T*2 site; from the X-ray data, Al becomes progressively more evenly distributed between *T*2 and *T*3 sites. The increase in sodium produces some cavities containing Na_4Cl, with a charge of +3 (Fig. 12). This is balanced by three neighboring AlO_4 tetrahedra. The extra silicon introduces flexibility in the ordering of the *T*2-*T*3 chains, which allows for the distribution of aluminum between *T*2 and *T*3 sites, without the necessity of Al-O-Al bonds or more than two Al in any four-membered ring. The ^{29}Si nmr spectra show the two peaks from the 33% *Me* structure (Fig. 1) but also extra peaks due to *T*1 (4Si) at -110 ppm, *T*2-*T*3(2Si2Al) at -96 ppm and *T*2-*T*3(3Si1Al) at -101 ppm. These small peaks are not resolved in this spectrum and are observed as a raised baseline between the two main peaks.

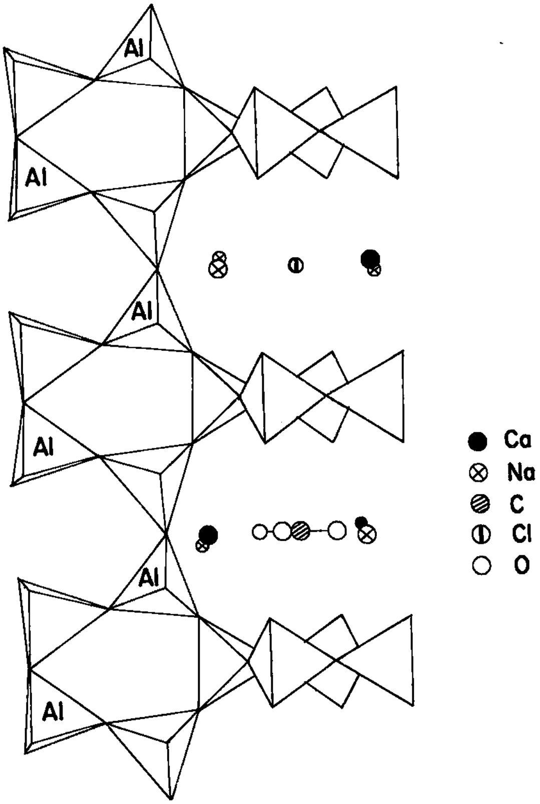

FIG. 11. Model of cation ordering in 33% *Me* scapolite.

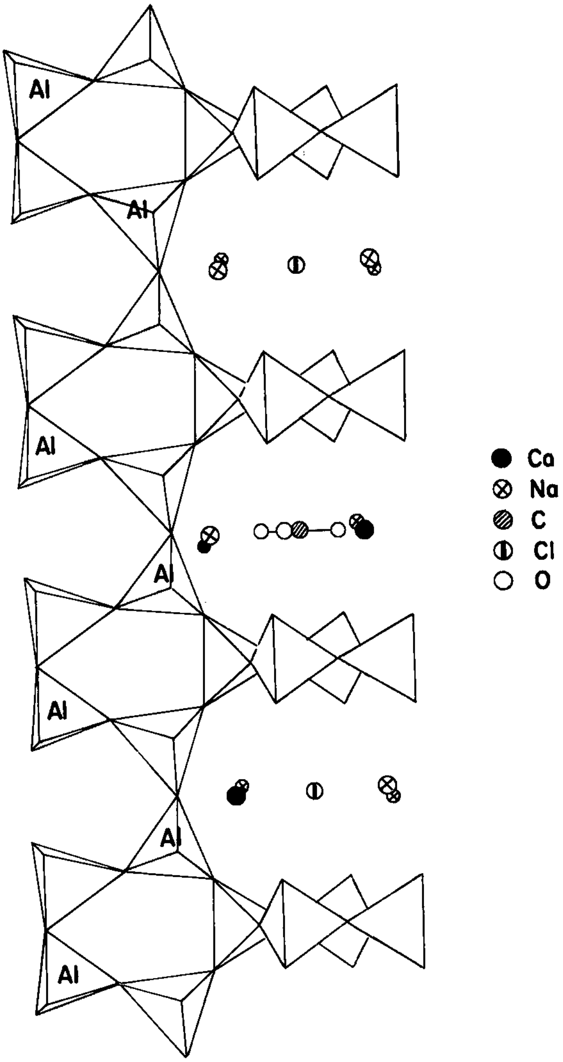

FIG. 12. Model of cation ordering in 20% *Me* scapolite.

With increasing meionite content beyond 33%, aluminum enters the *T*1 site. The change of one next-nearest-neighbor *T*1 from Si to Al is shown in the ^{29}Si nmr spectra by a progressive decrease in the peak due to *T*1(3Si1Al) at -106 ppm and a corresponding increase in the *T*1(2Si2Al) peak at -101 ppm. There is also an increase in the intensity of the *T*2–*T*3(4Al) peak. The increase in negative charge around each cavity due to the extra Al is balanced by $NaCa_3CO_3$ and Ca_4CO_3 configurations, with charges of +6 and +5, respectively (Fig. 13).

At 70% *Me* each *T*1 ring can have one aluminum-bearing and three silicon-bearing tetrahedra, but in compositions more aluminous than 70% *Me* it is necessary to place two aluminum atoms into some *T*1 rings. This results in all cavities having a -5 or -6 charge, which cannot be balanced by Cl-containing clusters. Therefore there is virtually no Cl in the structure above 70% *Me*.

Two aluminum ions in a *T*1 ring produce *T*1(1Si3Al) peaks at -96 ppm and *T*1(4Al) peak at -91 ppm at the expense of the other *T*1 peaks. There is the expected large difference in the spectra beyond 70% *Me*, which correlates with 2 aluminum atoms entering a *T*1 ring. There is also a steady increase in the size of the *T*2–*T*3(4Al) peak.

The anticipated relative intensities of the peaks were calculated from this model and found to correlate well, within experimental error, with the measured intensities (Table 8).

Aluminum-27 MAS nmr

There is an increase in the width of the ^{27}Al with increasing meionite content, with an additional increase of about 200 Hz between 44% and 48% *Me* (Fig. 3). Below 37% *Me*, aluminum occurs only in

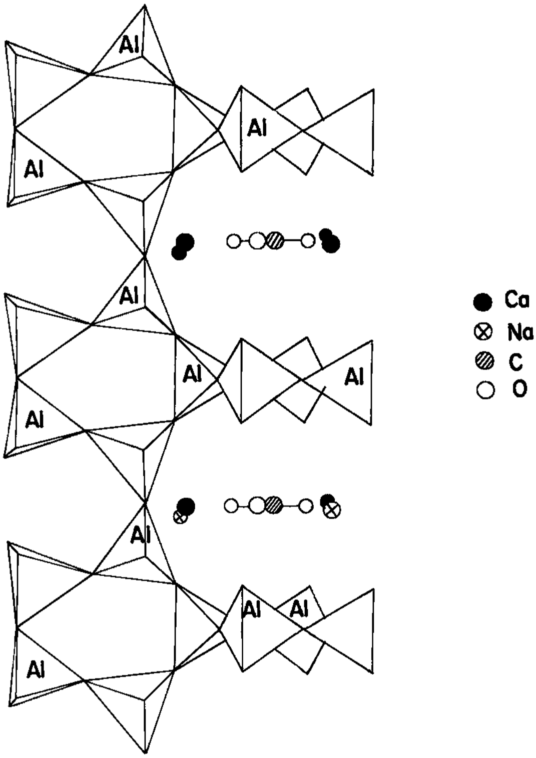

FIG. 13. Model of cation ordering in 75% *Me* scapolite.

TABLE 8. NUMBER OF SILICON ATOMS IN EACH T CONFIGURATION

Sample		T2/3 (4AL)	T2/3 (3AL)	T1 (3AL)	T2/3 (2AL)	T1 (2AL)	T2/3 (1AL)	T1 (1AL)	T1 (0AL)
ON8	(a)	0.2	2.3	-	1.3	-	0.5	3.4	0.8
	(b)	0.2	2.8	-	1.0	-	0.3	3.5	0.4
	(c)	-	2.9	-	0.8	-	0.7	3.3	0.8
TANZ	(a)	0.2	3.1	-	0.7	-	0.4	3.3	0.4
	(b)	0.3	3.0	-	0.5	-	0.3	3.7	0.1
	(c)	-	3.6	-	0.3	-	0.1	3.9	0.2
ON7	(a)	-	3.8	-	-	0.2	-	4.0	-
	(b)	0.2	3.9	-	-	-	-	3.9	-
	(c)	-	4.0	-	-	-	-	4.0	-
MAD	(a)	0.2	3.8	-	-	0.7	-	3.1	-
	(b)	0.2	3.6	-	-	1.0	-	2.8	-
	(c)	0.4	3.6	-	-	0.5	-	3.2	-
Q13	(a)	0.9	2.9	0.2	-	1.1	-	2.4	-
	(b)	1.2	2.7	0.2	-	0.8	-	2.5	-
	(c)	0.5	3.5	-	-	0.8	-	2.9	-
MIN	(a)	0.4	3.6	-	-	1.3	-	2.2	-
	(b)	0.2	4.0	-	-	1.2	-	2.0	-
	(c)	0.7	3.3	-	-	1.0	-	2.5	-
BOLT	(a)	0.2	3.9	-	-	1.5	-	1.5	-
	(b)	0.8	3.0	-	-	1.6	-	1.6	-
	(c)	1.1	2.9	-	-	1.8	-	1.4	-
ON47	(a)	0.7	3.0	-	0.7	1.6	-	0.8	-
	(b)	1.0	2.3	-	1.0	1.8	-	1.0	-
	(c)	1.2	2.6	-	0.5	1.5	-	0.8	-
MONT	(a)	0.7	3.1	-	1.0	1.1	-	0.4	-
	(b)	1.5	2.1	-	1.4	1.1	-	0.3	-
	(c)	1.8	2.2	-	1.5	0.5	-	0.3	-

(a) Integrals measured by cutting around the peaks and weighing them
(b) Integrals measured from deconvolution of spectra
(c) Calculated values from model

the *T*2–*T*3(4Si) sites. Above 37% *Me*, aluminum entering the *T*1 site will also produce *T*1(4Si), *T*1(3Si1Al), *T*2(3Si1Al) and *T*3(3Si1Al) aluminum sites. Below 45% *Me*, less than 6% of the aluminum is in the *T*1 sites, which would give too low an intensity to affect peak width.

The specimens from amphibolite-facies metamorphic rocks of the Grenville Province lie on two linear trends (Fig. 3). Specimens from other environments deviate from this trend, indicating a different degree of Al–Si order.

Sodium-23 MAS nmr

In the scapolite structure, sodium is in asymmetrical eight-fold co-ordination, with seven oxygen atoms from the tetrahedral framework and one chlorine or oxygen from a carbonate or sulfate group (Fig. 14). Sodium–anion distances in the polyhedra vary from 2.35 to 3.02 Å (Lin & Burley 1973a) (Fig. 15).

The relatively symmetrical peak at −14.7 ppm of the ^{23}Na spectrum of ON9 (21.3% *Me*) (Fig. 4) is apparently due to sodium adjacent to chlorine, and the peak at −15.7 ppm from MONT (91% *Me*), to sodium adjacent to a carbonate group.

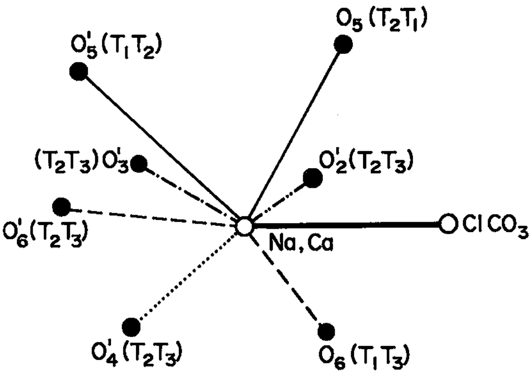

FIG. 14. Configuration of the Na–O polyhedron.

The shoulder at −20 ppm in the spectra of scapolite containing between 33 and 45% *Me* eludes a definite interpretation. One possibility is that increased asymmetry of the sodium sites in this compositional range produces additional quadrupolar distortion or shift in some of the ^{23}Na peaks. The asymmetry can be seen from a plot of (Ca,Na)–O distance against meionite content (Fig. 15). Bond distances between alkali cation and O2, O3 and O4 do not vary significantly across the series. (Na,Ca)–O5 and (Ca,Na)–O6 diverge by up to 0.20 Å between 33% and 50% *Me* but converge toward both endmember compositions. The change in the ^{23}Na MAS nmr spectra at about 45% *Me* corresponds to the composition at which there is a sudden increase in the width of the ^{27}Al MAS nmr peak.

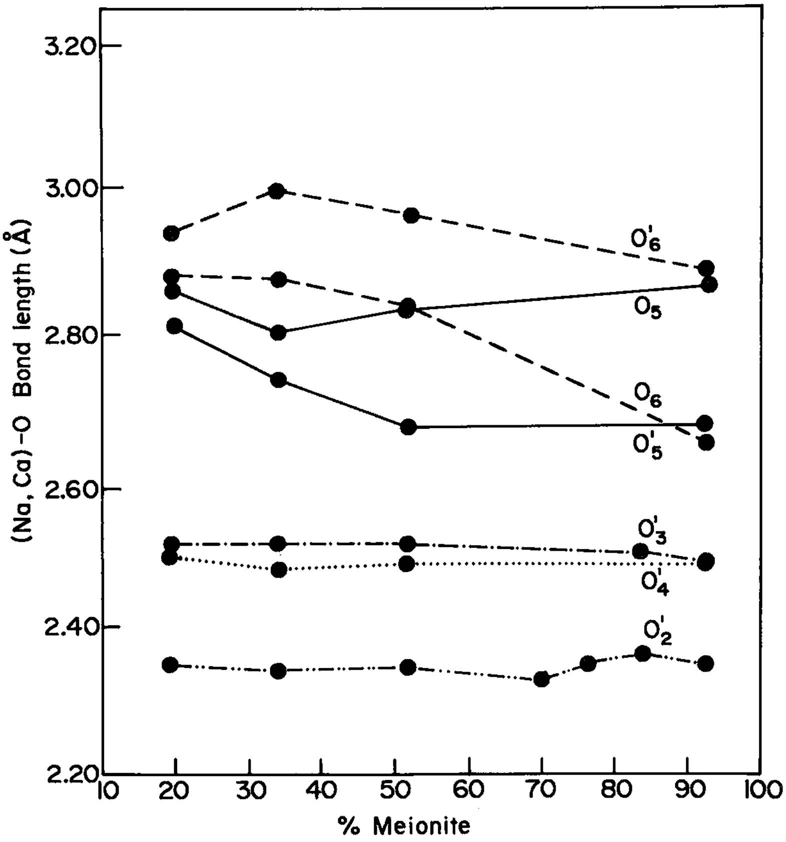

FIG. 15. A plot of (Na,Ca)–O distances as a function of meionite content.

Carbon-13 MAS nmr

The carbonate group in scapolite is planar, tilted less than 3° out of the (001) plane (Levien & Papike 1976), and occupies one of eight equivalent sites (Aitkin *et al.* 1984). In our model, the carbonate group is surrounded by four calcium ions, or by one sodium and three calcium or by two sodium and two calcium ions, in order to balance the negative charge on the aluminosilicate framework around the cavity.

The weak, broad ^{13}C peaks are shifted to the high field of other carbonate minerals (Table 5). There is a suggestion of a slight peak-shift across the series, but at the present level of instrumental resolution this cannot be definitely assigned to different carbonate environments. Aragonite resonates at 170.0 ppm, calcite, at 168.3 ppm, and magnesite, at 171.7 ppm.

CONCLUSION

Care is necessary in the correlation of X-ray data and nmr spectra for aluminum and silicon sites in disordered systems because X-ray data are an average of silicon and aluminum sites, whereas the nmr spectra are specific to either aluminum or silicon.

The ^{29}Si MAS nmr spectra of scapolite are complicated by the overlap of the peaks from *T*1 sites with *T*2 and *T*3 peaks with one more aluminum atom as next-nearest neighbor, but the spectra are sufficiently well resolved to give a clear indication of the state of Al–Si order in the structure and to lead to an allocation of most peaks to specific sites. This leads to a model for Al–Si ordering in which the charge on the cage is balanced locally by the requisite number of AlO_4 tetrahedra. In this model there is a maximum of two aluminum atoms in any four-membered ring and in these, aluminum atoms alternate with silicon atoms; however, the five-membered rings do contain Al–O–Al bonds at high concentrations of the meionite component.

*T*2–*T*3 chains remain internally ordered, with the apparent disorder of Al between *T*2 and *T*3 sites in compositions greater than 33% *Me*, indicated by previous X-ray work, explained by the rotation by 180° of individual *T*2–*T*3 chains relative to one another (*i.e.*, interchange of Al from *T*2 to *T*3). With less than 33% *Me*, the excess silicon in the *T*2–*T*3 chains allows for a change of Al occupancy from the *T*2 to *T*3 site to occur along a chain.

All of the *T*1 sites are occupied by silicon below 33% *Me*. With increasing aluminum content beyond 33% *Me*, firstly one Al enters each *T*1 ring, and then, beyond 70% *Me*, a second Al enters the *T*1 rings. At this point Cl-containing cavities can no longer be locally charge-balanced, and Cl is eliminated from the structure.

ACKNOWLEDGEMENTS

We thank the Natural Sciences and Engineering Research Council of Canada for financial support in the form of operating grants to HDG and JSH and a scholarship to BLS. Dr. R.E. Lenkinski and Mr. W. Klimstra are thanked for assistance with the instrumentation, the Southwestern Ontario High-Field NMR Centre for instrument time, Dr. C.A. Fyfe for the design of the MAS probe, and Professor D.M. Shaw of McMaster University and D. Moecher of the University of Michigan at Ann Arbor for samples of scapolite.

REFERENCES

AITKIN, B.G., EVANS, H.T., JR. & KONNERT, J.A. (1984): The crystal structure of synthetic meionite. *Neues Jahrb. Mineral. Abh.* **149**, 309-324.

BARRON, P.F. & FROST, R.L. (1985): Solid state ^{29}Si nmr examination of the 2:1 ribbon magnesium silicates sepiolite and palygorskite. *Amer. Mineral.* **70**, 758-766.

CHAMBERLAIN, C.P., DOCKA, J.A., POST, J.E. & BURNHAM, C.W. (1985): Scapolite: alkali atom configurations, antiphase domains, and compositional variations. *Amer. Mineral.* **70**, 134-140.

EVANS, B.E., SHAW, D.M. & HAUGHTON, D.R. (1969): Scapolite stoichiometry. *Contr. Mineral. Petrology* **24**, 293-305.

FYFE, C.A., GOBBI, G.C., HARTMAN, J.S., LENKINSKI, R.E., O'BRIEN, J.H., BEANGE, E.R. & SMITH, M.A.R. (1982): High resolution solid state MAS spectra of ^{29}Si, ^{27}Al, ^{11}B and other nuclei in inorganic systems using a narrow bore 400 MHz high resolution nmr spectrometer. *J. Magn. Resonance* **47**, 168-178.

______, ______ & KENNEDY, G.J. (1983): Investigation of the dealumination of zeolite ZSM-5 by solid state magic-angle spinning nmr. *Chem. Lett.*, 1551-1554.

______, ______, ______, DE SCHUTTER, C.T., MURPHY, W.J., OZUKBO, R.S. & SLACK, D.A. (1984): Chemical shift dispersion due to crystallographic inequivalence and implications regarding the interpretation of the high resolution ^{29}Si MAS nmr spectra of zeolites. *Chem. Lett.*, 163-166.

GROBET, P.J., MORTIER, W.J. & VAN GENECHTON, K. (1985): Influence of the cation distribution in zeolites on the isotropic ^{29}Si nmr chemical shift. *Chem. Phys. Lett.* **119**, 361-364.

JANES, N. & OLDFIELD, E. (1985): Prediction of silicon-29 nuclear magnetic resonance chemical shifts using a group electronegativity approach: applications to silicate and aluminosilicate structures. *J.Amer.Chem.Soc.* **107**, 6769-6775.

KIRKPATRICK, R.J., KINSET, R.A., SMITH, K.A., HENDERSON, D.M. & OLDFIELD, E. (1985): High resolution solid state sodium-23, aluminum-27 and silicon-29 nuclear magnetic resonance spectroscopic reconnaissance of alkali and plagioclase feldspars. *Amer. Mineral.* **70**, 106-123.

LEVIEN, L. & PAPIKE, J.J. (1976): Scapolite crystal chemistry: aluminum-silicon distributions, carbonate group disorder, and thermal expansion. *Amer. Mineral.* **61**, 864-877.

LIN, S.B. (1971): *The Crystal Structure and Crystal Chemistry of Scapolites.* Ph.D. thesis, McMaster Univ., Hamilton, Ontario.

______ & BURLEY, B.J. (1973a): Crystal structure of a sodium and chlorine-rich scapolite. *Acta Cryst.* **B29**, 1272-1278.

______ & ______ (1973b): The crystal structure of meionite. *Acta Cryst.* **B29**, 2024-2026.

______ & ______ (1975): The crystal structure of an intermediate scapolite-wernerite. *Acta Cryst.* **B31**, 1806-1814.

LIPPMAA, E., MAGI, M., SAMOSAN, A., ENGELHARDT, G. & GRIMMER, A.-R. (1980): Structural studies of silicates by solid state high-resolution ^{29}Si nmr. *J. Amer. Chem. Soc.* **102**, 4889-4893.

______, ______, ______, TARMAK, M. & ENGELHARDT, G. (1981): Investigation of the structure of zeolites by solid-state high-resolution ^{29}Si nmr spectroscopy. *J. Amer. Chem. Soc.* **103**, 4992-4996.

______, SAMOSAN, A. & MAGI, M. (1986): High resolution ^{27}Al nmr of aluminosilicates. *J. Amer. Chem. Soc.* **108**, 1730-1735.

LOWENSTEIN, W. (1954): The distribution of aluminum in the tetrahedra of silicates and aluminates. *Amer. Mineral.* **39**, 92-96.

MAGI, M., LIPPMAA, E., SAMOSAN, A., ENGELHARDT, G. & GRIMMER, A.-R. (1984): Solid state high resolution silicon 29 chemical shifts in silicates. *J.Phys. Chem.* **88**, 1518-1522.

Newton R.C. & Goldsmith, J.R. (1975): Stability of the scapolite meionite ($3CaAl_2Si_2O_8 \bullet CaCO_3$) at high pressures and storage of CO_2 in the deep crust. *Contr. Mineral. Petrology* **49**, 49-62.

Papike, J.J. & Stephenson, N.C. (1966): The crystal structure of mizzonite, a calcium- and carbonate-rich scapolite. *Amer. Mineral.* **51**, 1014-1027.

______ & Zoltai, T. (1965): The crystal structure of a marialite scapolite. *Amer. Mineral.* **50**, 641-655.

Peterson, R.C., Donnay, G. & Lepage, Y. (1979): Sulfate disorder in scapolite. *Can. Mineral.* **17**, 53-61.

Radeglia, R. & Engelhardt, G. (1985): Correlation of Si–O–T (T= Si or Al) angles and ^{29}Si nmr chemical shifts in silicates and aluminosilicates. Interpretation by semi-empirical quantum chemical considerations. *Chem. Phys. Lett.* **114**, 28-30.

Shaw, D.M. (1960a): The geochemistry of scapolite. I. Previous work and general mineralogy. *J. Petrology* **1**, 218-260.

______ (1960b): The geochemistry of scapolite II. Trace elements, petrology and general geochemistry. *J. Petrology* **1**, 261-285.

Sherriff, B.L. & Hartman, J.S. (1985); Solid-state high-resolution ^{29}Si nmr of feldspars: Al–Si disorder and the effects of paramagnetic centres. *Can. Mineral.* **23**, 205-212.

Received August 6, 1986, revised manuscript accepted March 7, 1987.